Strong quasi-simultaneous coupling of fluid-structure interaction in offshore applications

Veldman, Arthur; Seubers, Jan; Hosseini Zahraei, S. M.; van der Plas, Peter; Wellens, P.R.

Strong quasi-simultaneous coupling for fluid-structure interaction in offshore applications

Arthur E.P. Veldman[a*], Henk Seubers[a], Matin Hosseini Zahraei[b], Peter van der Plas[a], Peter Wellens[b]

[a] Bernoulli Institute for Mathematics, Computer Science and Artificial Intelligence, University of Groningen, The Netherlands

[b] Department of Ship Hydrodynamics, Delft University of Technology, The Netherlands

[*] Corresponding author: a.e.p.veldman@rug.nl

1 Introduction

Simulating the hydrodynamics of deformable, floating structures using a partitioned strategy poses a major challenge when the physical coupling between the fluid and the structure is strong and the ratio of the added mass to the structural mass is considerate. In numerical simulations of such systems with two-way interaction numerical instabilities can occur, which do not occur in systems with inherently one-way interaction. Existing computational procedures for fluid-structure interaction become less efficient or even unstable. In these situations, it is advisable to modify the coupling to allow the fluid to respond better to the body motions. A simultaneous solution of the equations governing fluid and (solid or elastic) body would be a stable choice, but is often not feasible. Usually the numerical problems are taken care of with sub-iterations between fluid and structure, but their convergence can be slow; e.g. [Causin et al., 2005, Forster et al., 2006].

In this paper we present a more powerful, *quasi-simultaneous* approach, which tries to mimic a fully simultaneous coupling in an affordable way as introduced by Veldman for aerodynamic viscous-inviscid boundary-layer interaction [Veldman, 1981, Veldman, 2009]. In our application, the quasi-simultaneous approach makes use of a simple approximation (termed *interaction law*) of the elastic-body dynamics, based on the (6 DOF) solid-body modes and the main elastic modes of the structure.

The fluid solver in this study is the symmetry preserving finite-volume VOF method ComFLOW [Kleefsman et al., 2005, Veldman et al., 2007, Wemmenhove et al., 2015]. A finite element method is used to solve the elastic structure response based on a Euler-Bernoulli beam. Kinematic and dynamic relations couple fluid dynamics to the structural dynamics.

2 Mathematical model

Flow model Incompressible, turbulent fluid flow can be modeled by means of the Navier–Stokes equations

$$M\mathbf{u} = 0, \qquad \frac{\partial \mathbf{u}}{\partial t} + C(\mathbf{u})\mathbf{u} + Gp - V\mathbf{u} = \mathbf{f}. \tag{1}$$

Here M is the divergence operator, which describes conservation of mass. Conservation of momentum is based on the convection operator $C(\mathbf{u})\mathbf{v} \equiv \nabla(\mathbf{u} \otimes \mathbf{v})$, the pressure gradient operator $G = \nabla$, the viscous diffusion operator $V(\mathbf{u}) \equiv \nabla \cdot \nu \nabla \mathbf{u}$ and a forcing term $\mathbf{f}$. The kinematic viscosity is denoted by ν. The flow equations are discretized on a staggered grid with a finite-volume method. The convective terms are discretized in a skew-symmetric energy-preserving way [Verstappen and Veldman, 2003]. Also the discrete pressure gradient G is the negative transpose of the discrete divergence operator M, such that also the pressure does not influence the energy balance.

The free-surface location is indicated by a Volume-of-Fluid [Hirt and Nichols, 1981] function ϕ, and reconstructed by means of Youngs' PLIC method [Youngs, 1987, Düz, 2015].

In this exposition, for simplicity reasons the first-order forward Euler time integration will be used. In the actual calculations, a second-order Adams–Bashforth method is being applied.

The solution of the discrete Navier–Stokes equations is split into two steps. Firstly, an auxiliary variable $\tilde{\mathbf{u}}$ is introduced

$$\Omega \frac{\tilde{\mathbf{u}} - \mathbf{u}^n}{\delta t} = -\mathsf{C}(\mathbf{u}^n)\,\mathbf{u}^n + \mathsf{V}\mathbf{u}^n + \mathbf{f}, \quad \text{such that} \quad \mathbf{u}^{n+1} = \tilde{\mathbf{u}} - \delta t\, \Omega^{-1} \mathsf{G} \mathsf{p}^{n+1}. \tag{2}$$

Secondly, by imposing discrete mass conservation at the new time level, substitution of (2) results in a discrete Poisson equation for the pressure:

$$\delta t \, \mathsf{M}_0 \Omega^{-1} \mathsf{G} \mathsf{p}^{n+1} = \mathsf{M}_0 \tilde{\mathbf{u}} + \mathsf{M}_\Gamma \mathbf{u}_\Gamma^{n+1}, \tag{3}$$

where M_0 and M_Γ represent the discrete continuity operator in the interior and along the boundary, respectively.

Structural model For simplicity, in this study the structure is selected to be a one dimensional Euler–Bernoulli beam. Assuming a constant cross section A for the beam, its equation of motion is

$$\rho_s A \frac{\partial^2 d}{\partial t^2} + EI \frac{\partial^4 d}{\partial s^4} = f, \tag{4}$$

with appropriate initial and boundary conditions. Here, s denotes a coordinate along the beam, d the beam deformation, ρ_s the beam density, E Young's modulus, I the second moment of inertia and f the load per unit length of the beam.

The structural response of the elastic body (eb) is modeled with a finite element method. Omitting the technical details, the resulting discrete set of equations can be written in the form

$$\mathsf{M}_{\text{eb}} \ddot{\mathsf{d}} + \mathsf{K}_{\text{eb}} \mathsf{d} = \mathsf{f}, \tag{5}$$

where M_{eb} is the discrete mass operator and K_{eb} the discrete stiffness operator. These matrices can be simultaneously diagonalized as $\mathsf{Q}^T \mathsf{M}_{\text{eb}} \mathsf{Q} = \mathsf{I}$ and $\mathsf{Q}^T \mathsf{K}_{\text{eb}} \mathsf{Q} = \Lambda$, where Q contains the normalized elastic body eigenvectors (modes) with eigenvalues Λ. In this way, the elastic body dynamics (5) can be rewritten as

$$\mathsf{Q}^{-1} \ddot{\mathsf{d}} + \Lambda \mathsf{Q}^{-1} \mathsf{d} = \mathsf{Q}^T \mathsf{f}. \tag{6}$$

The temporal integration of the structure equations is performed by means of the generalized-α method [Chung and Hulbert, 1992].

Fluid-solid interface The coupling relations along the fluid-solid interface Γ_{FS} consist of two relations: the kinematic and the dynamic conditions. The kinematic condition states that the motion of the interface on both sides matches. The dynamic condition expresses equilibrium of stresses at the fluid-solid interface.

3 Numerical coupling

Time marching with sub-iterations Information has to be exchanged between the two subsystems: the fluid solver provides the loads to the structural solver, whereas in return the latter provides the structural motion to the flow solver. In an explicit, weak coupling this exchange only happens once per time step, but this process is unstable for larger mass ratios. Therefore often per time step sub-iterations with severe under-relaxation (e.g. Aitken [Forster et al., 2006]) are introduced to achieve a strong coupling between the subsystems; Fig. 1(left). The convergence of this process can be rather slow, and each iteration a solid-fluid solve has to be performed. This makes this coupling method inefficient. In the next section we will present a method that shares the strong coupling with the above sub-iterations, but at a limited additional computational effort.

Quasi-simultaneous coupling For two-way coupled problems, a monolithic or simultaneous approach is not always possible, as the sub-domain solvers have to be coupled at a deep iterative level. In this section we will describe an approach that tries to combine the simplicity of a hierarchical coupling approach with the iterative power of a monolithic approach. In the quasi-simultaneous method, an approximation of the body dynamics is solved simultaneously with the fluid. This *interaction law* anticipates the body response in advance of the actual solid dynamics computation. As such, the interaction law (Fig. 1(right)).

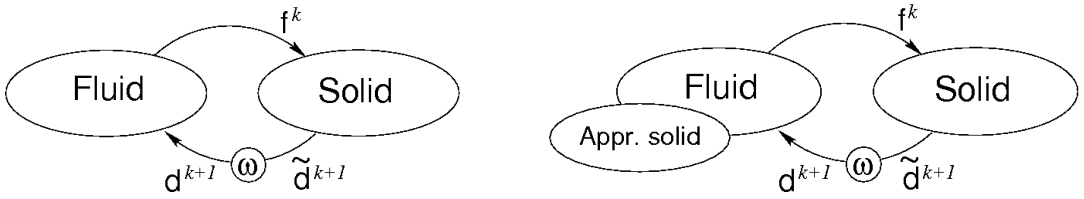

Fig. 1: (Left) Sub-iterative loop of FSI with relaxation within one time step; (right) adding an approximate interaction law. Force f, displacement d, whereas k is iteration level.

To understand the coupling stability, it is useful to formulate the coupling problem in terms of interface variables only: the velocity along the interface $\mathbf{u}_\Gamma$ (related to the displacement d, and the load exerted by the fluid to the structure $\mathbf{f}_\Gamma$ (for an elastic body found from the local stresses, for a solid body found from their integration along the interface).

Elastic body coupling

Because the structural equation (6) contains both $\ddot{\mathsf{d}}$ and d, first a discrete time integration is carried out. Thereafter, the discrete version of the hierarchically coupled problem at the new time level can be denoted as

$$\text{Elastic body } \mathsf{Q}^{-T}\left(\frac{\mathsf{I}}{\delta t^2}+\Lambda\right)\mathsf{Q}^{-1}\mathbf{d}_\Gamma^{k+1}=\mathbf{f}_\Gamma^k, \quad \text{Fluid } \mathbf{f}_\Gamma^{k+1}=-\frac{\mathsf{M}_{\text{ad}}}{\delta t^2}\mathbf{d}_\Gamma^{k+1}. \tag{7}$$

The contribution from the previous time steps is omitted in view of clarity; it is just an inhomogeneous term in the right-hand side, which is not relevant for the convergence of the sub-iterations per time step.

The displacement $\mathbf{d}^{k+1}$ can be eliminated from the system of equations (7), after which the iterative process can be written as

$$\mathbf{f}^{k+1}=-\mathsf{M}_{\text{ad}}\mathsf{Q}(\mathsf{I}+\delta t^2\Lambda)^{-1}\mathsf{Q}^T\mathbf{f}^k. \tag{8}$$

For small enough δt, the amplification factor simplifies to $-\mathsf{M}_{\text{ad}}\mathsf{Q}\mathsf{Q}^T$, where $\mathsf{Q}\mathsf{Q}^T$ has the dimension of $1/kg$. Thus we recognize again an added-mass ratio, leading to divergence when the added mass of the fluid is too large.

In the quasi-simultaneous treatment we approximate the behavior of the elastic body by a simple reduced-order model consisting of a limited number of modes, including the solid-body modes. Let these be collected in the matrix $\tilde{\mathsf{Q}}$. Thus, the proposed interaction law reads

$$\mathbf{d}^{k+1}-\widetilde{\mathsf{Q}}\left(\frac{1}{\delta t^2}+\widetilde{\Lambda}\right)^{-1}\widetilde{\mathsf{Q}}^T\mathbf{f}^{k+1}=\left\{\mathsf{Q}\left(\frac{1}{\delta t^2}+\Lambda\right)^{-1}\mathsf{Q}^T-\widetilde{\mathsf{Q}}\left(\frac{1}{\delta t^2}+\widetilde{\Lambda}\right)^{-1}\widetilde{\mathsf{Q}}^T\right\}\mathbf{f}^k. \tag{9}$$

Letting $\delta t\to 0$, i.e. studying zero-stability, and combining with the fluid-flow model (7), the quasi-simultaneous iterative process reduces to

$$\mathbf{f}^{k+1}=-(\mathsf{M}_{\text{ad}}^{-1}+\widetilde{\mathsf{Q}}\widetilde{\mathsf{Q}}^T)^{-1}(\mathsf{Q}\mathsf{Q}^T-\widetilde{\mathsf{Q}}\widetilde{\mathsf{Q}}^T)\mathbf{f}^k. \tag{10}$$

Clearly, if all of the modes are incorporated into the interaction law, the spectral radius will become zero and the method simultaneously solves the fluid with the 'exact' body.

Implementation

The interaction law is a relation between the pressure and the local velocity of the body surface. This relation can be substituted in the right-hand side of the discrete Poisson equation (3) and thus can be considered as a boundary condition. It can be shown that the latter retains its favorable numerical properties (symmetric, negative definite), such that its iterative solution can proceed as before.

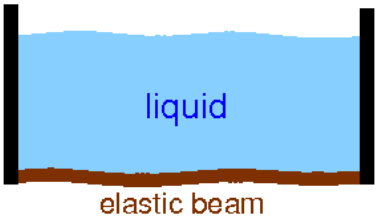

Fig. 2: Schematic of the first test case; the domain with free-surface flow on top and flexible beam at the bottom

4 Examples

Elastic body: tank with membrane bottom

In order to assess the performance of the quasi-simultaneous approach for different mass ratios, a test case has been designed in which this ratio can be varied.

At the bottom of a rectangular container ($1.0 \times 0.1 \times 0.5\,\mathrm{m}^3$) filled with 50 kg of water, a flexible beam is placed as illustrated in Fig.2. The mass of the beam is varied between 1 kg and 50 kg; its module of elasticity is 1 MPa. The interaction law is made out of truncated structural modes; the number of modes dictates its accuracy. The relaxation parameter is adjusted by Aitken's method. Five cases with different mass ratios are solved with and without the interaction law. Also, the effect of the accuracy of the interaction law on the performance is studied.

First, the effect of the added mass ratio is studied. The interaction law is constructed out of the first 10 modes, while the symmetry of the problem cancels out the effect of odd modes. For all the cases the initial relaxation parameter is set to 1, while from the third FSI iteration this value is adjusted by Aitken's method. Fig. 3 shows the convergence of the FSI iterations during the first time step. As shown in Fig. 3(left), higher mass ratios require more computational effort. Plugging in the interaction law, Fig. 3(right) reproduces the same solution while the computational effort is less. It can be observed that the difficult cases with higher mass ratios speed-up a lot more from the quasi-simultaneous approach than the easier cases with modest mass ratios. The difference in convergence rates is clearly visible, with the quasi-simultaneous method hardly needing any under-relaxation.

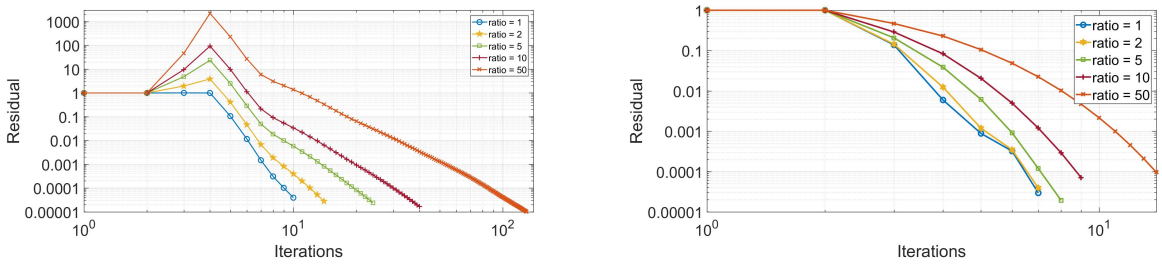

Fig. 3: Convergence history for the first time step for different added mass ratios: (left) without interaction law, (right) with interaction law.

Next, the effect of the number of modes in the interaction law is shown in Fig. 4. Obviously, employing more modes improves the structure response estimation in the interaction law. But there is a trade off, as the gain goes down while making the interaction law itself more expensive. When the mass ratio is low, the number of effective modes is lower than the case when mass ratio is 50.

Rubber gate

The validation test case is an elastic rubber gate placed in front of a bulk of water. This experiment has been performed by Antoci [Antoci et al., 2007]. The gate separating the fluid from the air is partly rigid, but the lower part is elastic. The rubber gate is clamped on the top side and free on the other side. The density of the beam is $\rho_s = 1100$ kg/m^3 and the Young modulus for elasticity is $E = 10$

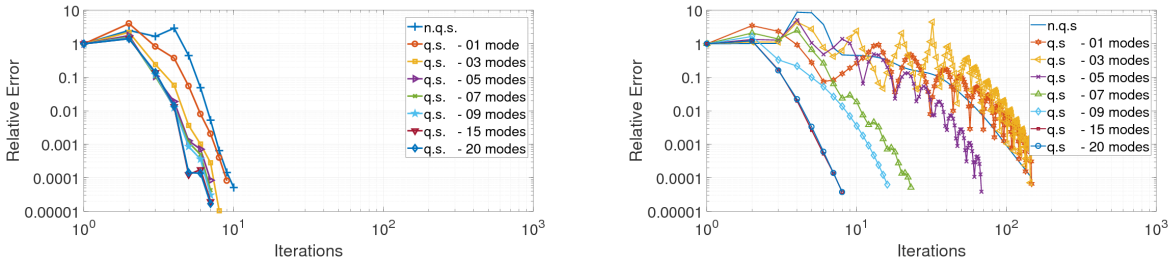

Fig. 4: Convergence history for the first time step for varying accuracy (number of included modes) of the interaction law: (left) mass ratio 1; (right) mass ratio 50.

MPa. According to [Antoci et al., 2007], the problem is mostly two dimensional, so in the current study numerical simulations are performed in 2D. A grid of $250 \times 2 \times 50$ is used. The initial time step is set to be 1×10^{-4}; this value is automatically adjusted during the simulation based on the Courant condition.

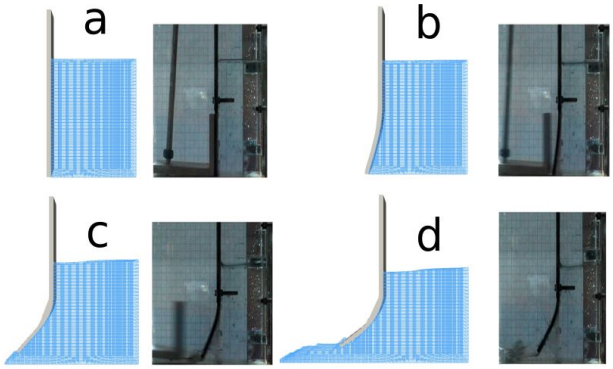

Fig. 5: Snapshots of the simulation past a rubber gate, compared with the experiment of [Antoci et al., 2007]

The results after 0.12 s, with the snapshots from experiment and simulation at time intervals of 0.4 s, are compared in Fig. 5.

5 Conclusion

It has been demonstrated that the ratio of the fluid added mass versus the solid-body mass is an important parameter controlling the (in)stability of a fluid-structure system. Whereas traditional (sub-)iteration methods require severe under-relaxation, a quasi-simultaneous method can handle large added mass ratios more efficiently. An interaction law approximating the structural dynamics is its key ingredient. It is shown that only a couple of dominant modes are needed to achieve a stable method. The stability and resulting efficiency has been demonstrated by comparing the computational effort with and without interaction law on a number of offshore-related applications.

6 Acknowledgments

This work is part of the research programme Maritime2013 with project number 13267 which is (partly) financed by the Netherlands Organization for Scientific Research (NWO).

References

Antoci, C., Gallati, M., and Sibilla, S. (2007). Numerical simulation of fluidstructure interaction by SPH. *J. Comp. Struct.*, 85:879–890.

Causin, P., Gerbau, J. F., and Nobile, F. (2005). Added-mass effect in the design of partitioned algorithms for fluid-structure problems. *Comp. Meth. Appl. Mech. Eng.*, 194:4506–4527.

Chung, J. and Hulbert, G. M. (1992). A time integration algorithm for structural dynamics with improved numerical dissipation: the generalized-α method. *J. Appl. Mech.*, 60(2):371–375.

Düz, B. (2015). *Wave generation, propagation and absorption in CFD simulations of free surface flows*. PhD thesis, Technical University Delft.

Forster, C., Wall, W. A., and Ramm, E. (2006). Artificial added mass instabilities in sequential staggered coupling of nonlinear structures and incompressible viscous flows. *Comp. Meth. Appl. Mech. Eng.*, 196:1278–1293.

Hirt, C. W. and Nichols, B. D. (1981). Volume of fluid (VOF) method for the dynamics of free boundaries. *J. Comput. Phys.*, 39:201–25.

Kleefsman, K. M. T., Fekken, G., Veldman, A. E. P., Iwanowski, B., and Buchner, B. (2005). A Volume-of-Fluid based simulation method for wave impact problems. *J. Comput. Phys.*, 206:363–393.

Veldman, A. E. P. (1981). New, quasi-simultaneous method to calculate interacting boundary layers. *AIAA J.*, 19:79–85.

Veldman, A. E. P. (2009). A simple interaction law for viscous-inviscid interaction. *J. Eng. Math.*, 65:367–383.

Veldman, A. E. P., Gerrits, J., Luppes, R., Helder, J. A., and Vreeburg, J. P. B. (2007). The numerical simulation of liquid sloshing on board spacecraft. *J. Comput. Phys.*, 224:82–99.

Verstappen, R. W. C. P. and Veldman, A. E. P. (2003). Symmetry-preserving discretization of turbulent flow. *J. Comput. Phys.*, 187:343–368.

Wemmenhove, R., Luppes, R., Veldman, A. E. P., and Bunnik, T. (2015). Numerical simulation of hydrodynamic wave loading by a compressible two-phase flow method. *Computers & Fluids*, 114:218–231.

Youngs, D. L. (1987). An interface tracking method for a 3d Eulerian hydrodynamics code. Technical Report AWRE/44/92/35, Atomic Weapons Research Establishment.